Supplement of Biogeosciences, 20, 3539–3553, 2023
https://doi.org/10.5194/bg-20-3539-2023-supplement

Biogeosciences Open Access EGU

Supplement of

Sources and sinks of carbonyl sulfide inferred from tower and mobile atmospheric observations in the Netherlands

Alessandro Zanchetta et al.

Correspondence to: Huilin Chen (huilin.chen@rug.nl, huilin.chen@nju.edu.cn)

S1 Observed deviations from seasonal cycles by wind directions during stationary measurements

Figure S1 shows the deviation of the COS, CO_2 and CO mole fractions from their seasonal cycle for the Lutjewad site against wind direction. A negative (positive) deviation (e.g., $COS_{7m} - COS_{seas.} < 0$) is indicative of a sink (source) that is not represented by the seasonal cycle. Typically, there is a difference in signals between daytime and strongly stable nights, especially for deviations of 7 m mole fractions (left plots in Figure S1). No large COS deviations are observed for daytime data and weakly turbulent nights (when the temperature gradient between 60 and 7 m is lower than 0.75 °C), apart from a decrease of ~ 15 ppt with wind from the east (see Figure S1a-b). For nighttime data with strongly stable conditions, we observe larger deviations from the seasonal cycle. For 7 m deviations we generally observe the largest depletions in COS from eastern wind and southwestern wind, which is with wind from inland (wind directions between 50 – 300º). However, no clear depletions are observed with wind directions from the south. For 60 m (right plots in Figure S1) we also find COS to be depleted in eastern wind directions (Figure S1b), and see weak depletions for winds from the southwest. COS mole fractions were substantially lower at all heights in a period of a few days between 1 and 8 September 2014 (not shown).

For CO_2 and CO, we observe elevations from the seasonal cycle for both day and night. The elevations span the range of wind directions for which air originates from land. The CO_2 mole fractions are further enhanced in the nighttime. The CO elevations are similar for day and nighttime, apart from a peak at 200 degrees, which is higher during strongly stable conditions.

Peaks at night do not necessarily point to larger sources or sinks in a certain direction, but could originate from a few nights with strongly stable conditions that drive large changes in mole fractions and that have a relatively large influence on the averages. The binned averages of the strongly stable nighttime conditions are more prone to such peaks because these data represent less data (332 data points) than the weakly stable nights (1269 data points).

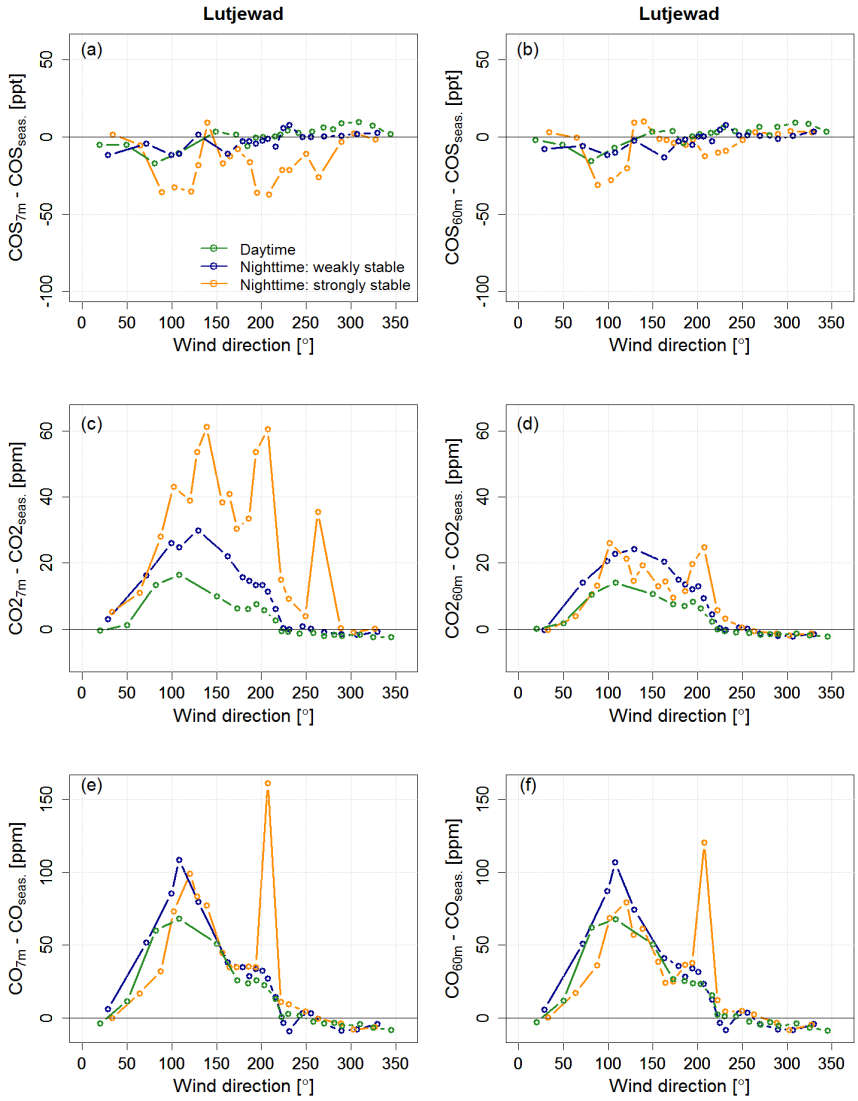

Figure S1: Deviation of 7 m (left) and 60 m (right) mole fractions of COS (a,b), CO_2 (c,d) and CO (e,f) from their seasonal cycle in Lutjewad. Data are separated between daytime (solar elevation angle > 0°; green) and nighttime (solar elevation angle < 0°), where nighttime data are divided over weakly (blue) and strongly (orange) stable nights, which are separated based on the temperature difference between 60 and 7 m being smaller or larger than 0.75 °C.

S1.1 Spatial distribution of COS and CO_2 sources and sinks

The wind direction analysis in Figure S1 aids in identifying the main sources and sinks of COS in the region of the Lutjewad measurement station, although we have to consider that sources and sinks can balance each other. In general, we find depletions of COS only coming from inland, which is likely driven by terrestrial vegetation and soil. This last, in particular, was measured to be a COS sink during nighttime, as reported in Section 3.1. In wind directions from the North, we did not observe a deviation from the seasonal cycle, indicating that the mud flats and salt marshes are not a strong net source or sink of COS. Still, a source of COS in the salt marshes could be balanced by COS uptake from plants.

The fact that we observe COS depletion at 60 m during daytime is an indication that this is a regional signal rather than a local signal. The depletions of COS that we observe from the

southwest are larger at 7 m under strongly stable nighttime conditions than during daytime and at 60 m, which implies that these depletions are caused by more local sinks of COS. On average, we do not detect a sink from the south, even though this also covers continental air masses, including agricultural land nearby. Vegetative uptake of COS in this wind sector could be balanced by COS sources. The data in Figure S1 mainly represent the autumn and winter months with only the beginning and end of the growing season. Larger COS depletions can be expected in the summer months if vegetation plays a dominant role in the uptake of atmospheric COS.

The elevated CO_2 mole fractions during daytime likely originate from anthropogenic activities, which is substantiated by elevated CO mole fractions in the same range of wind directions. In the nighttime we find CO_2 mole fractions to be further elevated than during the daytime, because the effects are amplified in a shallow mixing layer. In both cases, we cannot attribute these elevations to anthropogenic sources alone because the net ecosystem exchange (NEE) of CO_2 can contribute significantly to these elevations. Other tracers, e.g. $^{14}CO_2$, are needed to partition the CO_2 elevations into anthropogenic emissions and NEE (Turnbull et al., 2009; van der Laan et al., 2010; Vogel et al., 2010). The wind directions where CO_2 enhancements at 7 m shows a peak in the night (200º and 275º) are also the wind directions where COS depletions are larger, and for one of the two peaks there is also a CO peak (200º). We are not aware of any anthropogenic activity that could lead to depletions of COS and at the same time emit CO_2 and CO. The sources and sinks of these gases do therefore not have to be related. We also have to consider that wind directions may differ at 7 and 60 m, especially during the night. Moreover, a few nights with strongly stable conditions and a particular wind direction could have a large influence on the averages, which would affect all gases and would be detected as a peak.

S2 Seasonal fit

A non-linear least squares fit was made to the 60 m COS mole fractions from Lutjewad, see Figure S2. The shape of the fit is represented by a harmonics function after Thoning et al. (1989, eq. 1 therein). We used the highest available heights, such that the mole fractions are the least affected by local influences, and we selected only daytime data, such that the measured mole fractions are not influenced by the shallow nocturnal boundary layer. The seasonal fit of CO_2 (not shown) is based on continuous measurements of a co-located cavity ring-down spectrometer in 2014 and 2015 in Lutjewad. For the seasonal fit of CO_2, we selected only data with wind direction from the north (wind direction < 30 ° or > 260 °) to make sure that the data represent background air and are not affected by anthropogenic influences. This data selection was based on the wind direction analysis presented in Figure S1.

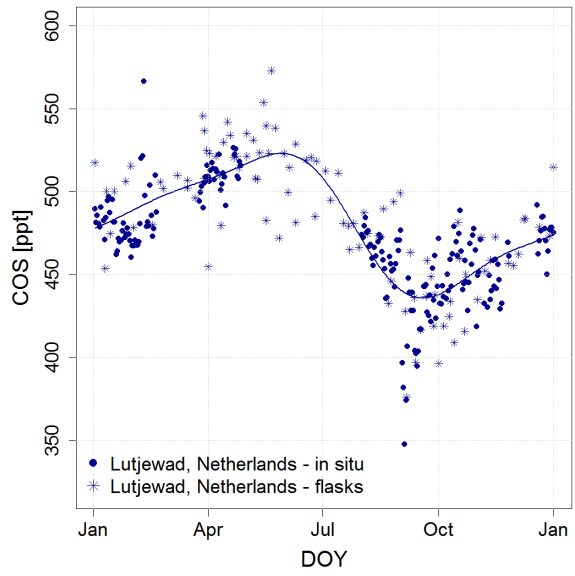

Figure S2: Seasonal cycle of daytime average COS mole fractions at 60 m in Lutjewad. The data consist of in-situ measurements from August 2014 – April 2015 and January – February 2018 (circles) and flask measurements between December 2013 and February 2016 (stars). The in-situ measurements from August 2014 – April 2015 are an update of the measurements presented in Kooijmans et al. (2016). The seasonal cycle shows a peak-to-peak amplitude of 87 ppt, which was estimated to be 96 ppt by Kooijmans et al. (2016) when no flask measurements were included.

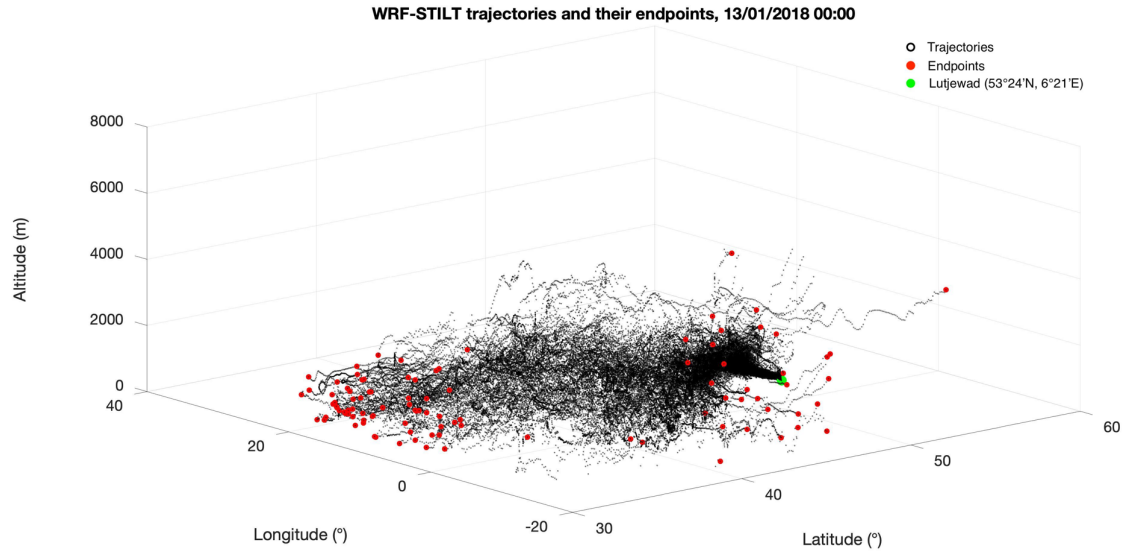

Figure S3: the trajectories of the 100 particles starting on 13/01/2018 00:00 from Lutjewad and their endpoints, according to the STILT model. Each endpoint (coloured in red) was associated to a COS boundary concentration following the TM5-4DVAR model (Ma et al., 2021). The average of these COS concentrations was used as the COS background for the simulation.

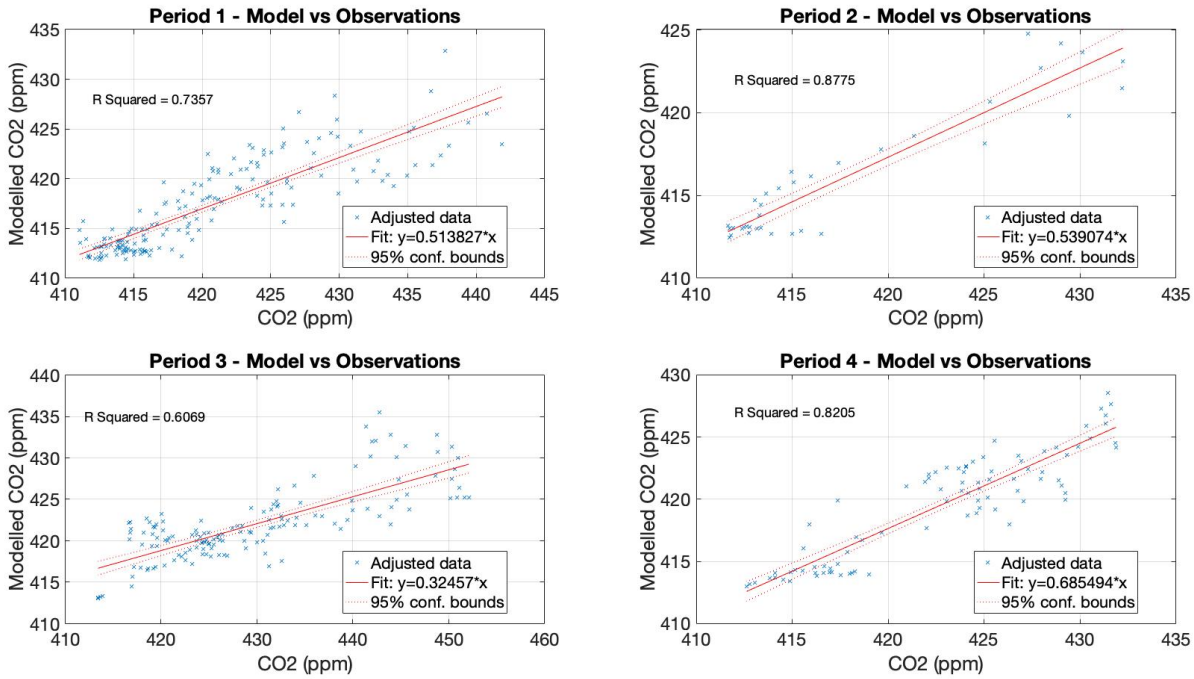

Figure S4: relationships between modelled CO_2 results and observations for the selected time periods.

5

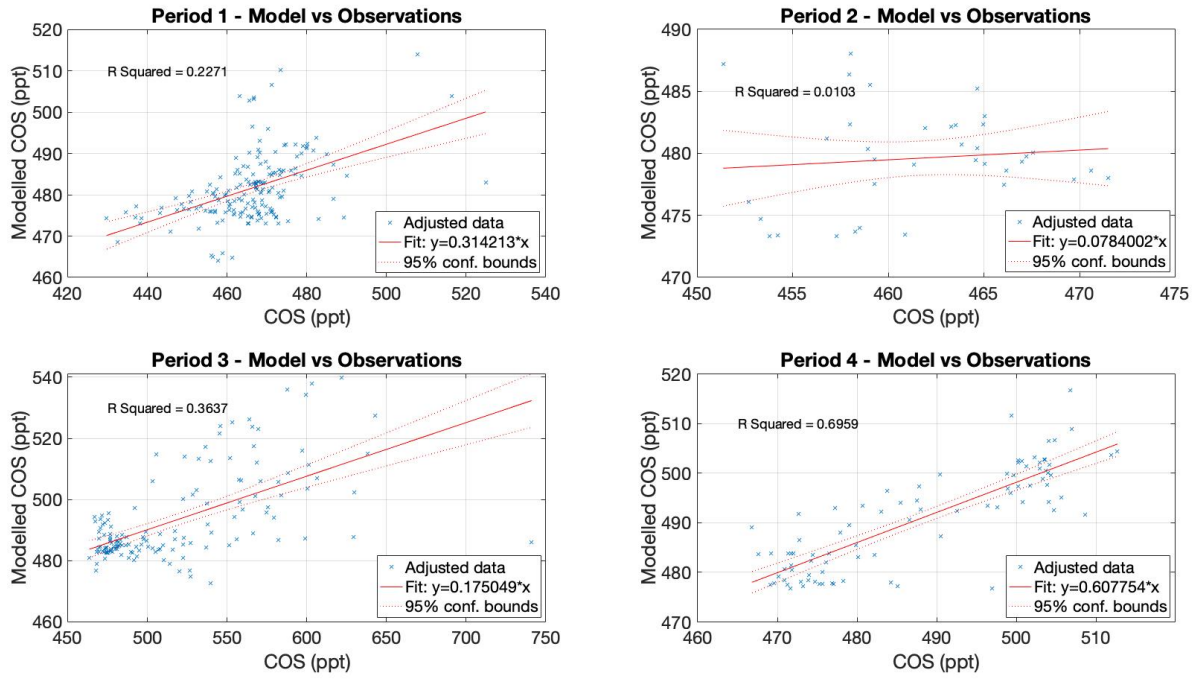

Figure S5: relationships between modelled COS results and observations for the selected time periods, where the only significant relationship is found for Period 4, identifying the source of these enhancements in the Ruhr region (Germany).

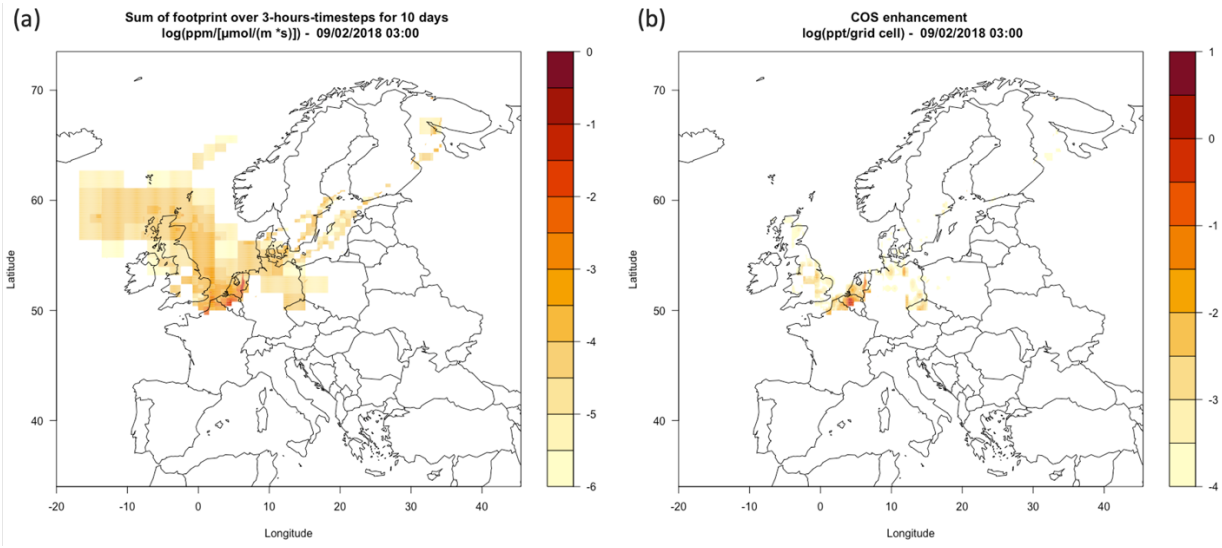

Figure S6: example of (a) footprint and (b) related COS enhancements for February 9th, 2018 (Period 3), retrieved as described in Sect. 2.4 in the main text (see also Figure 2). In this period, part of the measured COS enhancements could be attributed to the Antwerp-Rotterdam region.

Table S1: means ± standard deviations of gas species concentration for the samples collected in the Eemshaven area.

Sample origin	**COS (ppt)**	**CH_4 (ppb)**	**CO_2 (ppm)**	**CO (ppb)**	**N_2O (ppb)**
Sludge ponds	461 ± 21	2013.27± 0.79	411.74 ± 0.25	129.57 ± 0.47	333.94 ± 0.14
Sludge ponds	448 ± 13	2018.85± 0.35	411.58 ± 0.10	130.52 ± 0.59	333.91 ± 0.16
Coal storage	448 ± 17	2138.20± 0.49	409.53 ± 0.17	136.09 ± 0.51	333.93 ± 0.06
Coal storage	437 ± 13	2236.51± 0.37	472.96 ± 0.24	136.57 ± 0.88	333.95 ± 0.08
Wastewater	439 ± 9	2009.62± 0.71	406.34 ± 0.09	133.35 ± 0.46	333.71 ± 0.14
Wastewater	419 ± 6	2003.21± 0.19	405.14 ± 0.07	135.01 ± 0.33	333.61 ± 0.06
Background	424 ± 4	2008.63± 0.21	406.84 ± 0.08	136.62 ± 0.52	333.72 ± 0.07
Background	426 ± 8	2006.95± 0.33	407.38 ± 0.07	132.34 ± 0.52	333.55 ± 0.11

Table S2: means ± standard deviations of gas species concentration for the samples collected at the ATTERO facilities (Groningen).

Sample origin	**COS (ppt)**	**CH_4 (ppb)**	**CO_2 (ppm)**	**CO (ppb)**	**N_2O (ppb)**
Waste loading	534 ± 2	5396.52± 0.70	440.89 ± 0.09	136.38 ± 0.14	344.59 ± 0.05
Waste loading	473 ± 6	5659.73± 0.66	420.94 ± 0.17	139.01 ± 0.36	337.49 ± 0.08
Biodigesters	427 ± 9	3420.27± 1.34	433.47 ± 0.10	276.26 ± 0.14	334.12 ± 0.10
Biodigesters	429 ± 6	2494.50± 0.47	403.66 ± 0.54	163.59 ± 0.21	333.97 ± 0.12
Gas processing	425 ± 11	2636.08± 0.67	446.20 ± 0.14	141.62 ± 0.48	334.97 ± 0.16
Gas processing	435 ± 10	2321.13± 0.33	424.87 ± 0.16	135.54 ± 0.38	335.17 ± 0.13
Background	407 ± 21	2004.57± 0.57	403.27 ± 0.19	146.38 ± 0.49	334.57 ± 0.11
Background	413 ± 4	2008.74± 0.85	403.52 ± 0.18	150.21 ± 0.41	334.71 ± 0.12